◆ Human Brain Mapping 29:740–750 (2008) ◆

The Effect of Respiration Variations on Independent Component Analysis Results of Resting State Functional Connectivity

Rasmus M. Birn,* Kevin Murphy, and Peter A. Bandettini

Section on Functional Imaging Methods, Laboratory of Brain and Cognition, National Institute of Mental Health, NIH, Bethesda, Maryland

Abstract: The analysis of functional connectivity in fMRI can be severely affected by cardiac and respiratory fluctuations. While some of these artifactual signal changes can be reduced by physiological noise correction routines, signal fluctuations induced by slower breath-to-breath changes in the depth and rate of breathing are typically not removed. These slower respiration-induced signal changes occur at low frequencies and spatial locations similar to the fluctuations used to infer functional connectivity, and have been shown to significantly affect seed-ROI or seed-voxel based functional connectivity analysis, particularly in the default mode network. In this study, we investigate the effect of respiration variations on functional connectivity maps derived from independent component analysis (ICA) of resting-state data. Regions of the default mode network were identified by deactivations during a lexical decision task. Variations in respiration were measured independently and correlated with the MRI time series data. ICA appears to separate the default mode network and the respiration-related changes in most cases. In some cases, however, the component automatically identified as the default mode network was the same as the component identified as respiration-related. Furthermore, in most cases the time series associated with the default mode network component was still significantly correlated with changes in respiration volume per time, suggesting that current methods of ICA may not completely separate respiration from the default mode network. An independent measure of the respiration provides valuable information to help distinguish the default mode network from respiration-related signal changes, and to assess the degree of residual respiration related effects. *Hum Brain Mapp 29:740–750, 2008.*

Key words: default-mode network; respiration; independent component analysis; functional connectivity; rest

INTRODUCTION

A growing number of functional MRI (fMRI) studies are investigating not only the increase in fMRI signal with activation of particular brain areas, but also the correlation of time series fluctuations between brain regions. These studies are motivated by the observation that low frequency (<0.1 Hz) fluctuations in the MR signal intensity time series, which can occur either on top of task-induced signal modulations or in the absence of an external stimulus or explicit task, are often correlated between functionally related areas [Biswal et al., 1995; Cordes et al., 2000; Fox et al., 2007; Lowe et al., 1998; Rogers et al., 2007]. The general hypothesis is that these correlated fluctuations reflect synchronized variations in the neuronal activity of a network of regions. fMRI could therefore provide a window into the interaction, or connection, between brain

*Correspondence to: Rasmus M. Birn, Laboratory of Brain and Cognition, National Institute of Mental Health, 10 Center Dr., Bldg 10, Rm 1D80, Bethesda, MD 20892-1148. E-mail: rbirn@mail.nih.gov

Received for publication 2 November 2007; Revised 14 February 2008; Accepted 6 March 2008

DOI: 10.1002/hbm.20577

Published online 25 April 2008 in Wiley InterScience (www.interscience.wiley.com).

areas. The study of these networks by analyzing the coherent signal fluctuations has therefore become known as "functional connectivity" analysis.

The correlation between low frequency fluctuations in fMRI time series at rest (often referred to as a "resting state network," or "RSN") was first studied by Biswal et al. in the motor cortex [Biswal et al., 1995]. Subsequent studies have identified several consistent and distinct resting state networks, including motor, auditory, visual, and attention networks [Damoiseaux et al., 2006; De Luca et al., 2006]. Correlated fluctuations were also found between regions of the "default mode network"—a set of brain areas that consistently deactivate during a wide range of cognitive tasks [Greicius et al., 2003]. This supports the view that the brain at rest consists of a number of sporadically active and synchronized networks. Recent studies have also shown that the correlations within these resting-state networks, particularly the default mode network, can be altered in various neurological disorders, including schizophrenia [Garrity et al., 2007], Alzheimers' disease (Greicius et al., 2004b), ADHD [Sonuga-Barke et al., 2007], and autism [Cherkassky et al., 2006; Just et al., 2004, 2007; Muller, 2007].

The main challenge in analyses of functional connectivity is separating the neuronal-induced blood oxygenation level dependent (BOLD) fMRI signal changes from the many other sources of noise. For example, the heart beat and respiration can cause significant and correlated signal changes within and near large blood vessels and to a certain extent throughout gray matter [Biswal et al., 1996; Dagli et al., 1999; Lund et al., 2006]. These can be aliased to low frequencies at the typical imaging repetition times (TRs) of 1–2 s. Filtering out high frequencies (low-pass filtering) will therefore not remove all of this physiological noise [Bhattacharyya et al., 2004; Biswal et al., 1996]. Even at shorter TRs (e.g. 200–400 ms), the harmonics of the cardiac pulsations can alias into low temporal frequencies. Subject motion can also lead to coherent signal fluctuations, particularly at the edges of the brain or in areas of large spatial contrasts in signal intensity. Since these non-neuronal mechanisms are some of the largest sources of structured noise in resting MR data, reducing their influence is crucial for studies of functional connectivity.

Several methods have been developed to reduce cardiac- and respiration-induced signal fluctuations. Most of these require a separate measurement of the breathing and heart beat [Glover et al., 2000; Hu et al., 1995; Josephs et al., 1997]. A commonly used method, RETROICOR, for example, fits a low-order Fourier series to the imaging data based on the phase of the cardiac and respiratory cycle at the time of each acquisition. A few methods have been developed to reduce cardiac- and respiratory-induced noise when these physiological signals have not been independently measured. Some of these require a fast sampling rate [Chuang et al., 2001], while others rely on the consistent spatial pattern of signal changes induced by the heart beat and the breathing motion [Beall et al., 2007; Perlbarg et al., 2007]

More recent studies have shown that slower breath-to-breath changes in respiration depth and rate can significantly affect the fMRI signal (Birn et al., 2006; Wise et al., 2004). These signal changes are believed to be caused in part by respiration-induced changes in arterial CO_2, a potent vasodilator. Natural variations in breathing during rest typically occur at frequencies of around 0.03 Hz (a cycle roughly every 30 s), overlapping with the low frequencies studied in functional connectivity. The resulting induced MR signal changes occur in and near large vessels, and in brain areas with a high resting blood volume, which overlap with many areas of the default mode network. The fluctuations are not removed by typical physiological noise correction routines, which focus on fluctuations at the primary cardiac and respiratory frequencies, and their harmonics. Because of this overlap in both frequency and spatial location, slow changes in respiration depth and rate were found in a previous study to significantly affect resting-state functional connectivity analysis of the default mode network [Birn et al., 2006].

The earlier study of the impact of respiration variations on the default mode network by Birn et al. investigated the functional connectivity to a seed region located in the posterior cingulate [Birn et al., 2006]. This technique is a common approach to compute functional connectivity, in which a particular voxel or region is chosen as a "seed" and the correlation of the seed with the rest of the brain is calculated. The advantage of this method is that the interpretation is relatively straightforward—the resulting map shows all of the brain areas that have similar temporal fluctuations as compared to seed region. However, non-neuronal fluctuations in the seed region, such as those induced by respiration, can lead to false correlations and connectivity maps that represent similar physiological noise rather than correlated neuronal fluctuations. An alternative measurement that is now being used more frequently to study functional connectivity is independent component analysis, or ICA [Calhoun et al., 2005; Kiviniemi et al., 2003; McKeown and Sejnowski, 1998; McKeown et al., 1998, 2003]. With ICA, statistically independent spatial maps and their associated time courses are extracted from the data. One advantage of this method is that a temporal model of activation is not needed. ICA is therefore a useful tool in resting-state studies where the task is unconstrained. The primary disadvantage of ICA is that it is often difficult to know whether a component represents true underlying neuronal activation or an artifact.

The goal of this study is to determine the effect of the relatively slow breath-to-breath changes in respiration depth and rate on functional connectivity maps derived from previously published, and commonly used, resting state ICA methods. Since these respiration-induced fluctuations occur at similar low frequencies and in similar brain regions as the default mode network, we hypothesize that the ICA component typically identified as representing the "default mode network" will have a significant contribution from and correlation with respiration variations.

METHODS

To test our hypothesis and investigate the effect of respiration changes on functional connectivity maps derived from ICA, we performed ICA on resting-state data from 10 subjects (9 Female, 30.2 ± 8.1 years old). The data were taken from a previous study in which a seed-ROI functional connectivity approach demonstrated significant overlap between respiration-induced signal changes and the default mode network [Birn et al., 2006].

Experimental Parameters

Ten normal, healthy, right-handed volunteers were scanned under an Institutional Review Board (IRB) approved protocol after obtaining informed consent. Time series of T2*-weighted echo-planar MR images were acquired on a 3 T General Electric (GE) Signa MRI scanner (Waukesha, WI) using an 8-channel GE receive coil with whole body RF excitation. Whole brain coverage was achieved using 27–28 sagittal 5 mm thick slices. (TR: 2000 ms, TE: 30 ms, flip angle: 90°, FOV: 24 cm, slice thickness: 5 mm, matrix: 64 × 64, 165 image volumes per time series).

Tasks

Each subject performed two types of experimental runs: (1) resting with their eyes closed, and (2) a lexical decision making task. In the lexical task, subjects were presented with either real words or non-words (e.g. "GREST"), and were asked to indicate by a button press whether the word was real or not. Words and non-words were presented in a blocked design (30 s task blocks alternated with 30 s rest periods). In each task block, words and non-words were presented in random order once every 2 s. Five task blocks were presented in each run, for a total imaging time of 330 s per run. Resting runs were also 330 s in duration. A total of two lexical task runs and two resting runs were performed in eight subjects. Two subjects completed only one of the resting runs, in addition to the two task runs.

Physiological Data

Subjects' heart beats were recorded using a pulse-oximeter placed on the left index finger. These pulse-oximeter waveforms were used to determine the phase of the cardiac cycle in which each MR images was acquired. To reduce errors in this measurement, subjects were instructed to refrain from moving their finger during the scan. Respiration was measured with a pneumatic belt positioned at the level of the abdomen. The signal from this belt was determined to be linearly related to the expansion of the belt. The cardiac and respiratory measurement devices are supplied by the scanner manufacturer (GE Medical Systems, Waukesha, WI), are integrated into the MR scanner, and synchronized to the image acquisition. Physiological waveforms are sampled every 25 ms, and recorded to a text file. While a more direct measurement of end-tidal CO_2 using a capnograph may provide a better correlation with MR signal changes induced by variations in respiration depth or rate, the respiration belt is easy to apply and is intergrated into the scanner. Cardiac and respiratory measurements were visually inspected for errors, such as spurious noise or failure of the recordings.

An estimate of the respiration volume per unit time (RVT) was obtained as described in [Birn et al., 2006]. The maxima and minima for each breath were determined from the respiration belt measurement. The series of maxima and minima were then each interpolated to the time of each image volume acquisition (i.e. even intervals of the repetition time, TR). The respiration period was determined by subtracting the time between successive maxima, and again this series of respiration periods was interpolated to the imaging TR. The time series of RVT changes was then computed by subtracting the minima from the maxima and dividing by the period for each imaging time point.

Data Analysis

Data were preprocessed using AFNI [Cox, 1996]. Reconstructed images were first corrected for motion using a rigid-body volume registration. Physiological noise correction was then performed using the RETROICOR technique [Glover et al., 2000]. This correction regresses out signal fluctuations time-locked with the phase of the cardiac and respiratory cycles, and reduces the signal oscillations at the primary cardiac and respiratory frequencies (~1.1 Hz and ~0.3 Hz, respectively), as well as their first harmonics, even when these frequencies are aliased. Motion parameters were also included in this regression step. Resting runs were then low-pass filtered at a cutoff of 0.1 Hz.

Activations and deactivations to the lexical task were determined by linear regression analysis. In this analysis, the task-induced response was modeled by the task timing convolved with a Gamma-variate hemodynamic response function ($\mathrm{irf}(t) = kt^r e^{-t/b}$ where k is a scaling factor, $r = 8.6$, and $b = 0.547$ [Cohen, 1997]). Both task runs were concatenated, and motion parameters estimated from the image registration were included as additional nuisance regressors. Groups maps of activations and deactivations we obtained by converting the t-statistics of the regression analysis to Z-scores, transforming these to Talairach coordinates, and averaging the Z-scores across subjects.

MR signal changes induced by variations in the respiration volume per unit time during the resting runs were estimated by linear regression analysis, with the RVT time course as the ideal regressor. Since the signal changes induced by variations in RVT exhibit a latency spread across voxels, the latency of the ideal regressor was allowed to vary for each voxel. This was accomplished by repeating the regression analysis 51 times (for shifts from −10 to 40 s in 1 s increments) and choosing for each voxel the latency that gave the best fit. Since periods of deeper breathing (larger RVT) generally result in decreased blood flow, and hence a decreased fMRI signal, the best negative

fit with the shifted RVT was chosen in each voxel. The amount of breathing variation was computed in each subject by dividing the standard deviation of the RVT by the mean RVT.

Independent component analysis of the resting runs were performed using the MELODIC program from the FMRIB Software Library (FSL) (www.fmrib.ox.ac.uk/fsl) [Beckmann et al., 2004]. The data were de-meaned, the variance normalized voxel-wise and whitened. The number of components (N) was estimated using the Laplace approximation to the Bayesian evidence of the model order [Minka, 2000]. The data were decomposed into a set of N time-courses and spatial maps by thresholding at the standard P-value of 0.5. To enable across-subject comparisons, the components were transformed into Talairach space onto a $2 \times 2 \times 2$ mm^3 grid.

Identification of Components

Components from the ICA analysis that likely represent either artifact or one of the resting state networks were first determined by visually inspecting all of the components. Following this, a more impartial measure of identifying specific components was used. Components that represent default mode network activity were determined more objectively in two ways: (1) spatially correlating each component with a mask derived from the deactivations for that particular subject (Individual-DMN), and (2) spatially correlating each component with a mask derived from the deactivations based on the group data from all 10 subjects (Group-DMN). These masks were obtained by thresholding the deactivations at a t-statistic of 4.8 (Bonferroni corrected $P < 0.01$) for the individual subject data and a Z-score of 2.0 for the group data. The component with the highest correlation to the deactivation map was taken as the component most likely to represent the "default mode network" resting-state correlations. ICA components that reflect signal changes induced by variations in the respiration were determined objectively in three ways: spatially correlating each component with a mask derived from regions that show a significant fit to the RVT time-course from either (1) the individual subject (Individual-RVT) or (2) the group data (Group-RVT); and (3) Computing the peak (minimum) of the correlation function between the time course associated with each component and the RVT time course (1D-RVT). This correlation function was determined by correlating the component time course and the RVT time course at 51 different time lags, from -10 to $+40$ s.

RESULTS

Identification of the Default Mode Network Using the Lexical Task

The lexical task resulted in consistent activations and deactivations in each subject. Activations were found primarily in the left and right precentral gyrus, middle occipital gyrus, fusiform gyrus, and inferior frontal gyrus. Deactivations were observed in the anterior cingulate, medial prefrontal cortex, posterior cingulate, precuneus, and the superior occipital gyrus (see Fig. 1a). These deactivation occur in regions typically shown to be part of the default mode network [Greicius et al., 2003; Raichle et al., 2001].

Respiration-Induced Signal Changes

Robust respiration measurements were obtained in all of the resting runs. The respiration volume per time, reflecting breath-to-breath changes in the depth and rate of breathing, varied on average by approximately 28.1% $\pm$ 11.8% in each subject. This value reflects the average standard deviation of the RVT measure across time; the error ($\pm$) is computed across subjects. This resulted in significant MR signal changes in the precuneus, cuneus, bilateral superior temporal gyrus, fusiform gyrus, and occipital cortex (see Fig. 1c). The changes in RVT occurred at a peak frequency of $\sim$0.03 Hz.

Functional Connectivity Analyses

As previously published, a seed-ROI based analysis of functional connectivity, using the region of deactivation in the posterior cingulate as the seed, found a significant overlap between the resulting functional connectivity map and the respiration-induced signal changes (Birn et al., 2006). This functional connectivity map contained the regions classically identified as the default mode network (the posterior cingulate, anterior cingulate, prefrontal regions, and inferior parietal areas), in addition to more widespread regions of the occipital cortex, cuneus, precuneus, superior temporal gyrus, and fusiform gyrus (see Fig. 1e,f). Many of these additional regions were not found to deactivate during the lexical task.

The independent component analysis identified between 17 and 36 components in each resting run.

Identification of ICA Components

The purpose of this study was to evaluate whether ICA can separate the DMN from respiration-related (RVT) changes on an individual subject basis. Rather than presenting all of the relevant components from each of the subjects (a very large number of images to show in a Figure), we will instead provide a summary of ability of ICA to separate these two components, and show examples of cases where the separation worked, and where it failed.

Upon visual inspection, ICA appeared to separate the default mode network from RVT-related changes in almost every resting run (see Fig. 2 for an example from one subject). In several (10 of 18) cases, however, the default mode network component was difficult to identify clearly, as there appeared to be several likely candidates none of which perfectly matched the typical default mode network pattern (i.e. the deactivations identified from the group

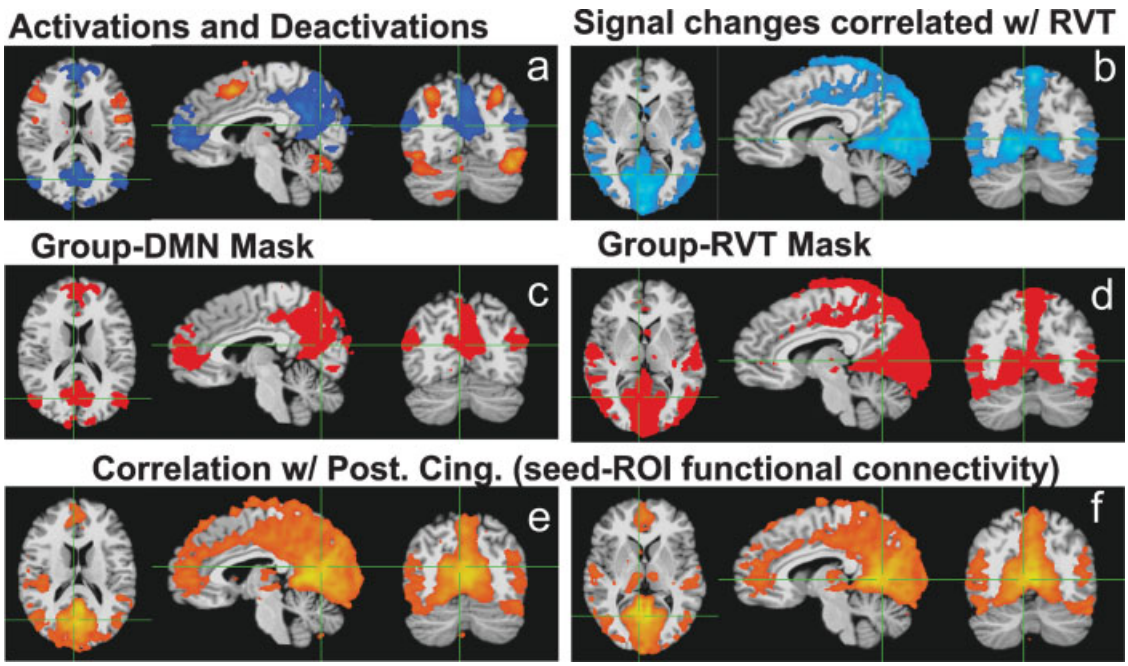

Figure 1.

(**a**) Activations (orange and yellow regions) and deactivations (blue regions) during the lexical task, from group data of 10 subjects (18 resting runs). Areas of deactivation correspond to regions frequently identified as the default mode network. (**b**) Signal changes significantly correlated with variations in the respiration volume per unit time (RVT), averaged over 10 subjects. (**c**) Mask derived from the deactivations. (**d**) Mask derived from significant RVT-related changes. (**e,f**) results of the seed-ROI based functional connectivity analysis. Colored regions indicate the voxels significantly correlated with the resting signal intensity time course averaged over the seed ROI. This seed ROI was defined by the areas showing a significant deactivation in the posterior cingulate during the lexical task. (e) maps at the same locations as figure a,c; (f) maps at the same locations as in Figures b,d.

data). RVT-related changes, characterized by a large posterior region of signal change (Fig. 2b), were more clearly identifiable (in 16 of 18 runs), appearing in one and occasionally two components. The frequency spectrum of the resting state default mode network and the RVT related changes appeared fairly similar, with both components showing peaks primarily below 0.05 Hz (Fig. 2e,f).

The more objective determinations of the default mode network and the respiration related components were generally consistent with the visual identification of components. In 14 of 18 runs, the component with the highest correlation to the individual-DMN mask (i.e. the component automatically identified as the "default mode network" in that subject) was different than the three components most correlated, either spatially or temporally, with the RVT (Fig. 2). In the remaining four cases, the component most correlated with the Individual-DMN mask was the same as the component most correlated with the respiration-induced changes (the Individual-Resp mask) (Fig. 3d).

In some cases the failure to correctly identify the default mode network using the Individual-DMN mask is due to a poor deactivation of that subject during the lexical task. In these subjects, only a few voxels primarily located near large vessels, such as the sagittal sinus, showed a robust deactivation. In three subjects, using masks based on the group deactivation (Group-DMN) instead identified a different component, which was more consistent with the visual identification of the default mode network, and which did not coincide with the components most correlated with respiration induced changes (Fig. 3c,d). However, in two other runs, the component identified as the default mode network using the group mask (Group-DMN) now coincided with the component most significantly correlated with respiration (Fig. 3a,b). In summary, in 3 of 18 runs, the automatically identified DMN component using the group masks coincided with the automatically identified RVT component.

Using the ICA component with the highest correlation to the deactivation maps created from either the individual subject or group maps to identify the default mode network is not a completely reliable method of automatic identification. In many cases, there were several ICA components with a similar correlation to the DMN mask. The component with the second or third highest correlation to this ideal mask was often the same as the component most correlated with respiration. In fact, in only one subject (two runs) were the three components most correlated with the DMN mask not among the three components

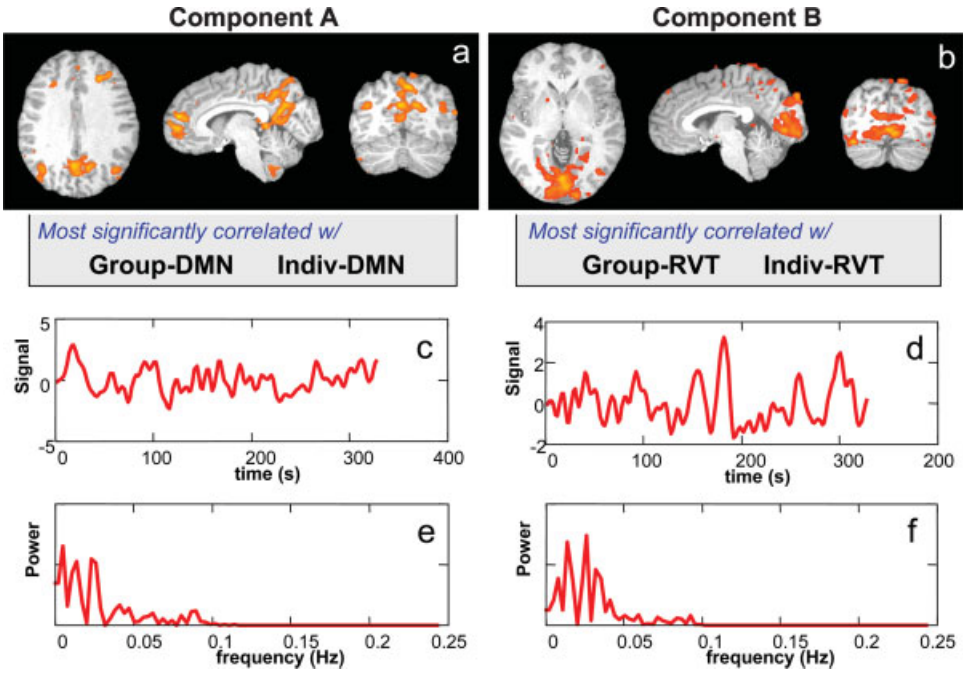

Figure 2.

Two components identified by ICA in one subject. (**a**) The Individual-DMN and Group-DMN masks were most highly correlated with the first component (Component A). (**b**) The Individual-RVT and Group-RVT masks were most highly correlated with the second component (Component B). This separation between DMN and RVT related components was observed in most (14/18) subjects. (**c,d**) Signal intensity time courses associated with each component. (**e,f**) Power spectrum of the signal intensity time courses shown in c,d. Both default mode network and respiration-related components have most of their power at low frequencies (<0.05 Hz).

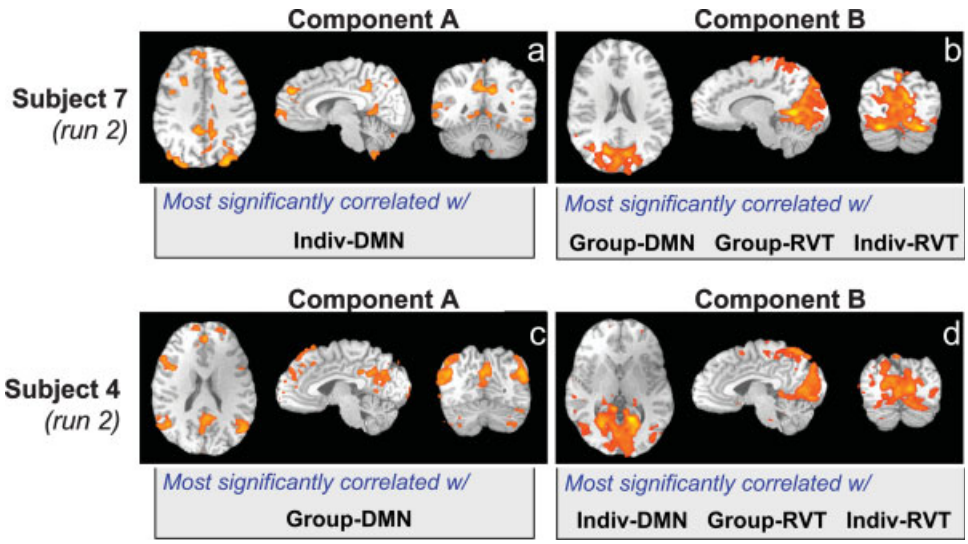

Figure 3.

Examples of ICA components from two subjects where either the Individual (**a**) or the Group (**b**) DMN mask was most highly correlated with a component that was also most highly correlated with both the Individual-RVT and Group-RVT masks. In these subjects, the automatic method of identifying the DMN instead chose a component that reflected respiration-related changes.

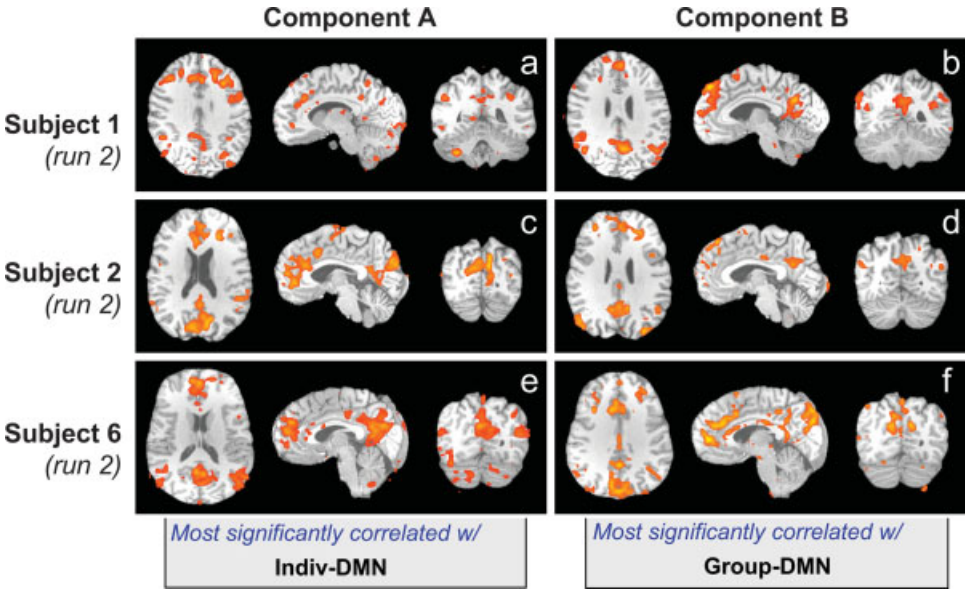

Figure 4.

Examples from three subjects where the Individual-DMN and the Group-DMN masks were correlated with different components. Each component has a pattern similar to the typical default mode network seen in the literature.

most correlated with the RVT. Additionally, in some cases there were multiple components that were visually similar to the expected default mode network, one of which was more highly correlated with the Individual-DMN mask, and another that was more highly correlated with the Group-DMN mask (see Fig. 4).

Finally, we looked at the temporal correlation between the RVT time course (within a range of latencies) and the time series associated with the various automatically identified components (see Table I). The average correlation coefficients were -0.51 ± 0.14 for the component most correlated with the Individual-RVT mask, and slightly lower, at -0.42 ± 0.23, for the Group-RVT mask. Correlations with the automatically identified default mode network components were also relatively high for some of the runs, with an average correlation coefficient of -0.26 ± 0.12 for the component most correlated with the Individual-DMN mask, and -0.25 ± 0.15 for the Group-DMN mask.

DISCUSSION

Previous studies have shown that the MRI signal changes induced by breath-to-breath changes in respiration depth and rate at rest occur at low temporal frequencies (<0.1 Hz), similar to the low frequency fluctuations presumed to reflect spontaneous neuronal activity, and at spatial locations that overlap with the default mode network [Birn et al., 2006; Wise et al., 2004]. On the basis of this, we hypothesized that ICA of resting data would have difficulty separating the default mode network activity from

TABLE I. Correlation coefficients between the respiration volume per time (RVT) time course obtained from the subject's respiration, and the time series associated with the component most correlated with various spatial masks—Individual-RVT, Group-RVT, Individual-DMN, and Group-DMN

	Indiv-RVT	Group-RVT	Indiv-DMN	Group-DMN
Subj 1, run 1	−0.41	−0.25	−0.08	−0.08
Subj 1, run 2	−0.19	0.28	0.19	0.25
Subj 2, run 1	−0.52	−0.52	−0.44	−0.44
Subj 2, run 2	−0.66	−0.64	−0.32	−0.51
Subj 3, run 1	−0.59	−0.59	−0.07	−0.07
Subj 4, run 1	−0.55	−0.49	−0.55	−0.55
Subj 4, run 2	−0.62	−0.62	−0.62	−0.37
Subj 5, run 1	−0.46	−0.55	−−0.36	−0.36
Subj 5, run 2	−0.57	−0.26	−0.16	−0.16
Subj 6, run 1	−0.50	−0.50	−0.23	−0.23
Subj 6, run 2	−0.68	−0.68	−0.34	−0.22
Subj 7, run 1	−0.37	−0.37	−0.28	−0.37
Subj 7, run 2	−0.37	−0.37	−0.12	−0.37
Subj 8, run 1	−0.63	−0.54	−0.31	−0.18
Subj 9, run 1	−0.59	−0.59	−0.59	0.02
Subj 9, run 2	−0.28	−0.17	−0.38	−0.38
Subj 10, run 1	−0.62	−0.47	−0.25	−0.25
Subj 10, run 2	−0.48	−0.30	−0.34	−0.34

Significant correlations (CC > 0.3, $P < 0.0001$) are highlighted in gray. The RVT time course is expected to correlate highly with components that appear spatially similar to areas that show significant RVT-related changes. However, even the time series from components that are most correlated with DMN masks, and not the most correlated with RVT masks, are significantly correlated with the RVT time course.

the respiration-induced changes. To test our hypothesis, we performed an independent component analysis on resting-state data where we had previously shown a seed-based functional connectivity analysis to be influenced by changes in respiration. We employed an ICA routine, MELODIC from the FMRIB Software Library (www.fmrib.ox.ac.uk/fsl), that has been frequently used on resting-state fMRI data [Beckmann et al., 2004; Damoiseaux et al., 2006; De Luca et al., 2006; Greicius et al., 2004a]. Contrary to our hypothesis, it appears that ICA can separate the default mode network from respiration related components in most cases. One or more components tend to match the areas that are typically deactivated during a demanding cognitive task, including the posterior cingulate, inferior parietal areas, the medial prefrontal region, and anterior cingulate (see Figs. 2a and 3a,c). Other components consistently derived using ICA include regions in the parietal and occipital cortex, extending inferior to the regions identified as the default mode network and overlapping with the areas correlated with respiration volume per time changes (see Figs. 2b and 3b,d).

This separation does not eliminate the need for physiological monitoring, as the predominant challenge of ICA is identifying what each component represents—which component reflects the default mode network activity and which component reflects respiration induced signal changes? In many studies, components are identified visually as representing a particular resting state network. In addition to being labor intensive, this visual identification method is somewhat subjective and difficult for other research groups to replicate. In this study we therefore looked at additional, more objective, ways to define the components.

Implicitly, a visual identification of components performs a spatial correlation with expectations or preconceptions based on previous group data. A more objective way to identify particular components, therefore, is a correlation with spatial mask defined from group data. The component representing correlated fluctuations within the default mode network, for example, was identified by spatially correlating each component with a mask derived from the group map of deactivations during the lexical task (the Group-DMN mask). Similarly, the component reflecting respiration-induced signal changes was identified by computing the correlation coefficient of each component with a spatial mask derived from a group average of regions significantly correlated with RVT changes. The advantage of using these group masks is that they generally reflect the spatial characteristics that we are interested in on a group level. In most cases, the Group-DMN mask chose a component that consisted primarily of regions traditionally considered to be part of the default mode network. In three cases, the mask was most correlated with possible respiration induced changes, and in two other cases, the mask chose a component that contained only a part of the traditional default mode network regions. An additional advantage of using group-defined masks is that the masks could be predefined without needing a separate run or analysis to determine the areas of deactivation or respiration-induced signal change. A shortcoming, of course, is that these group masks do not account for individual variability in the anatomy and location of function, or the individual variability in the amplitude and location of respiration induced signal changes.

An alternative method of automatically identifying relevant components is to calculate the correlation coefficient of each component with masks of signal changes derived from that particular subject, rather than a group average. These masks can account for individual subject differences in anatomy and function, and may therefore more closely match the components reflecting particular networks of correlated fluctuations. In some runs, the DMN component identified in this way was indeed more similar to the typical pattern of default mode network activity seen in the literature. In other runs, however, this mask identified components more likely due to respiration-induced signal changes. These failures can be the result of increased noise in the individual subject, compared to group, masks. Additionally, an individual subject may not deactivate during the lexical task, but still have resting correlations within the typically defined default mode network regions. In this case, a spatial correlation with a group mask would more accurately identify the default mode network.

Since a measure of the respiration is acquired in each subject, it may be more precise to look for a component that reflects the respiration-induced signal changes in that subject, rather than a component that contains the regions showing the largest signal changes over a group of subjects. Not surprisingly, the time courses associated with the spatial components identified in this manner (i.e. using the Individual-RVT masks) were more significantly correlated with that subject's RVT time course. In some cases, the Individual-RVT mask correlated best with components showing signal changes primarily in the motor cortex, while the component with the second-highest correlation consisted of an occipital region similar to that identified by the group map. This high correlation between the RVT changes and the motor cortex may be the result of a high resting blood volume in the areas of the motor cortex. Fluctuations in arterial CO_2 induced by changes in RVT will result in larger blood flow and blood oxygenation changes in regions with high resting blood volume. Alternatively, this component could be reflecting to the motor cortex activity associated with breathing (McKay et al., 2003). In other runs, the component most correlated with the Individual-RVT mask consists primarily of the sagittal sinus and voxels in the occipital cortex. These ICA components could reflect signal changes in large draining veins induced by changes in respiration.

While it appears that ICA separates the default mode network regions from respiration-induced changes in most cases, in some runs the component automatically identified as the default mode network was also the most highly correlated with respiration-induced changes. An additional

difficulty with this automatic identification of components comes in when there are several components with a similar correlation to the ideal mask. One of these could reflect the "true" default mode network activity, and another the respiration-induced changes. In these cases, having a separate physiological measure to determine which of the possible candidates of the default mode network likely reflects respiration-induced changes is clearly beneficial. This measure can also be used to determine the extent to which the component finally identified as the default mode network is correlated, either spatially or temporally, with changes in respiration.

The component most significantly correlated with the spatial map of signal changes related to variations in RVT consisted primarily of a region in the medial occipital cortex. This is similar to that identified by Damoiseaux et al. as the medial visual resting state network, one of the consistent resting state networks (RSNs) (Damoiseaux et al., 2006). It is possible, therefore, that this consistent RSN reflects primarily respiration-induced changes. Alternatively, the spatial locations of the respiration-induced changes and the medial visual activations may overlap by coincidence, and our method of identifying respiration-related changes by use of this spatial mask picks out a component that actually represents visual activation. The time course associated with this occipital component, however, is also highly correlated with RVT changes (see Table I, Group-RVT column). This ICA component, therefore, likely reflects at least a partial contribution from respiration-induced signal changes.

This study shows that in most cases the component best correlated with a spatial mask of default mode network regions is distinct from a component most correlated with respiration-related changes. However, does ICA (or, more precisely, the particular implementation of ICA used in this study) completely separate default mode network activity from respiration-related signal changes? In other words, is there a remaining contribution of respiration changes to the component identified as the default mode network? To assess this, we computed the correlation between the time series associated with component identified as representing fluctuations in the default mode network and the changes in respiration volume per time. In several cases, this correlation was almost as high as the correlation with the time series associated with the component identified as representing respiration-induced signal changes (see Table I). It is therefore possible that some contribution from respiration related signal changes remains in this component. An alternative possibility, which would be extremely difficult to disentangle, is that the default network is modulated by changes in respiration.

In the temporal correlation between the RVT time course and the component time course, we looked for the maximal negative correlation over a range of latencies. This negative correlation would reflect an increase in blood flow resulting from a decreased breathing depth (e.g. a brief breath-holding period), or conversely a decreased fMRI signal resulting from an increase in breathing depth or rate. Such a relationship is well-established. There have been a number of studies demonstrating, for example, that breath-holding results in an increase in the MRI signal [Abbott et al., 2005; Kastrup et al., 1998; Kwong et al., 1995; Li et al., 1999; Stillman et al., 1995; Thomason et al., 2005], that increases in the depth or rate of breathing cause a decrease in the fMRI signal [Birn et al., 2008], and that variations in $etCO_2$ are positively correlated with MRI signal changes [Wise et al., 2004]. While there are certainly known chemoreflex feedback mechanisms by which the levels of arterial CO_2 modulate the depth and rate of subsequent breaths (e.g. an increased arterial CO_2 level will result in an increased breathing depth or rate) [Guyton, 1986; Van den Aardweg et al., 2002], the effect of this feedback on the relation between breathing changes and MR signal changes has not been studied in detail.

Despite the growing popularity of functional connectivity analysis and the study of resting state networks, the source of these correlated fluctuations is not yet fully understood, and therefore many published interpretations are premature. Earlier studies have shown the influence of other noise sources, such as cardiac and respiratory fluctuations, which emphasizes the need for physiological corrections [Bhattacharyya et al., 2004; Birn et al., 2006; Biswal et al., 1996; Dagli et al., 1999; Lund, 2001; Wise et al., 2004]. An increasing number of studies, however, are showing that the correlated low-frequency fluctuations can indeed have a neuronal origin and may even have a behavioral significance [Fox and Raichle, 2007; Fox et al., 2007]. Studies using EEG, for example, have shown correlated fluctuations in specific frequency bands of the electrical activity between brain regions [Laufs et al., 2003]. Furthermore, direct recordings in nonhuman primates have also shown correlated local field potential (LFP) activity across the brain [Leopold et al., 2003; Vincent et al., 2007]. Low frequency fluctuations in resting-state fMRI data therefore likely represent some genuine underlying neuronal activity, provided that various non-neuronal confounds have been addressed.

The term "functional connectivity" is used to describe a variety of different analyses. Sometimes, it is computed from data that includes explicit task performance or an external stimulus; sometimes it is computed from the residual, after the task has been regressed out; and other times it is computed from resting data, where no explicit instructions are given. Maps of "connectivity" or "resting state networks" are generated either by correlation with a seed voxel or region, or with a data-driven method like ICA. What is important to remember is that all these analyses measure the (temporal) correlation between different brain regions. It does not necessarily imply a direct physical connection. This correlation can be caused by various mechanisms, including scanner artifacts, subject motion, cardiac and respiratory fluctuations, and correlated neuronal activity. Understanding the origins of these correla-

tions, and separating non-neuronal sources of signal fluctuations from neuronal sources, is critical for the proper interpretation of measures of functional connectivity as well as modulations in connectivity by activation or disease.

CONCLUSION

Signal changes induced by variations in the respiration depth and rate often occur at similar temporal frequencies and in similar locations as the default mode network. Even when traditional physiological corrections are applied, a seed-voxel or seed-ROI based resting-state functional connectivity analysis (e.g. with a seed in the posterior cingulate) can show strong correlations with regions outside of the typical default mode network (Birn et al., 2006). These unexpected correlations generally extend into the occipital cortex and include large vessels, such as parts of the Circle of Willis—regions that are highly correlated with changes in the respiration volume per unit time. In addition, the signal fluctuations induced by variations in breathing can result in either false negatives or false positives in task-related activation studies, particularly when the task is correlated with changes in respiration (Birn et al., 2006). Accounting for these physiological fluctuations is therefore of critical importance both for certain task-activation studies and the study of resting-state fluctuations.

In most cases, ICA separated these resting-state fluctuations into two or more components—one of which more closely resembled the default mode network typically discussed in the literature, and another that extended to a more inferior occipital region corresponding to the areas with the most significant respiration induced signal changes. The challenge is objectively identifying which component is most reflective of ongoing neuronal activity and connectivity, particularly when there are multiple components that reflect some aspects of either the default mode network or respiration related signal changes.

Three different methods (spatial correlation with group masks, spatial correlation with individual masks, or temporal correlation with the RVT time course) of automatically identifying the relevant components yielded slightly different results. Each one of the methods occasionally identified the component that that was most highly correlated with respiration-induced changes. Furthermore, and also troubling, was that the component automatically identified and most closely resembling the default mode network was still correlated to some degree with changes in the respiration volume per time. It is therefore possible that some of the current methods of ICA do not completely separate the two sources of signal change, and that this component still reflects to some degree, respiration-related signal changes. We demonstrate that, regardless of the method for identifying resting state networks an independent measure of the respiration provides valuable information to help distinguish the default mode network from respiration-related signal changes, and to assess the degree of residual respiration related effects.

REFERENCES

Abbott DF, Opdam HI, Briellmann RS, Jackson GD (2005): Brief breath holding may confound functional magnetic resonance imaging studies. Hum Brain Mapp 24:284–290.

Beall EB, Lowe MJ (2007): Isolating physiologic noise sources with independently determined spatial measures. Neuroimage 37: 1286–1300.

Beckmann CF, Smith SM (2004): Probabilistic independent component analysis for functional magnetic resonance imaging. IEEE Trans Med Imaging 23:137–152.

Bhattacharyya PK, Lowe MJ (2004): Cardiac-induced physiologic noise in tissue is a direct observation of cardiac-induced fluctuations. Magn Reson Imaging 22:9–13.

Birn RM, Diamond JB, Smith MA, Bandettini PA (2006): Separating respiratory-variation-related fluctuations from neuronal-activity-related fluctuations in fMRI. Neuroimage 31:1536–1548.

Birn RM, Smith MA, Jones TB, Bandettini PA (2008): The respiration response function: The temporal dynamics of fMRI signal fluctuations related to changes in respiration. NeuroImage 40:644–654.

Biswal B, Yetkin FZ, Haughton VM, Hyde JS (1995): Functional connectivity in the motor cortex of resting human brain using echo-planar MRI. Magn Reson Med 34:537–541.

Biswal B, DeYoe AE, Hyde JS (1996): Reduction of physiological fluctuations in fMRI using digital filters. Magn Reson Med 35:107–113.

Calhoun VD, Adali T, Stevens MC, Kiehl KA, Pekar JJ (2005): Semi-blind ICA of fMRI: A method for utilizing hypothesis-derived time courses in a spatial ICA analysis. Neuroimage 25:527–538.

Cherkassky VL, Kana RK, Keller TA, Just MA (2006): Functional connectivity in a baseline resting-state network in autism. Neuroreport 17:1687–1690.

Chuang KH, Chen JH (2001): IMPACT: Image-based physiological artifacts estimation and correction technique for functional MRI. Magn Reson Med 46:344–353.

Cohen MS (1997): Parametric analysis of fMRI data using linear systems methods. Neuroimage 6:93–103.

Cordes D, Haughton VM, Arfanakis K, Wendt GJ, Turski PA, Moritz CH, Quigley MA, Meyerand ME (2000): Mapping functionally related regions of brain with functional connectivity MR imaging. Am J Neuroradiol 21:1636–1644.

Cox RW (1996): AFNI: Software for analysis and visualization of functional magnetic resonance neuroimages. Comput Biomed Res 29:162–173.

Dagli MS, Ingeholm JE, Haxby JV (1999): Localization of cardiac-induced signal change in fMRI. Neuroimage 9(4): 407–415.

Damoiseaux JS, Rombouts SA, Barkhof F, Scheltens P, Stam CJ, Smith SM, Beckmann CF (2006): Consistent resting-state networks across healthy subjects. Proc Natl Acad Sci USA 103:13848–13853.

De Luca M, Beckmann CF, De Stefano N, Matthews PM, Smith SM (2006): fMRI resting state networks define distinct modes of long-distance interactions in the human brain. Neuroimage 29:1359–1367.

Fox MD, Raichle ME (2007): Spontaneous fluctuations in brain activity observed with functional magnetic resonance imaging. Nat Rev Neurosci 8:700–711.

Fox MD, Snyder AZ, Vincent JL, Raichle ME (2007): Intrinsic fluctuations within cortical systems account for intertrial variability in human behavior. Neuron 56:171–184.

Garrity AG, Pearlson GD, McKiernan K, Lloyd D, Kiehl KA, Calhoun VD (2007): Aberrant "default mode" functional connectivity in schizophrenia. Am J Psychiatry 164:450–457.

Glover GH, Li TQ, Ress D (2000): Image-based method for retrospective correction of physiological motion effects in fMRI: RETROICOR. Magn Reson Med 44:162–167.

Greicius MD, Menon V (2004a): Default-mode activity during a passive sensory task: uncoupled from deactivation but impacting activation. J Cogn Neurosci 16:1484–1492.

Greicius MD, Srivastava G, Reiss AL, Menon V (2004b): Default-mode network activity distinguishes Alzheimer's disease from healthy aging: Evidence from functional MRI. Proc Natl Acad Sci USA 101:4637–4642.

Greicius MD, Krasnow B, Reiss AL, Menon V (2003): Functional connectivity in the resting brain: A network analysis of the default mode hypothesis. Proc Natl Acad Sci USA 100:253–258.

Guyton AC (1986): Textbook of Medical Physiology. Philadelphia: Saunders.

Hu X, Le TH, Parrish T, and Erhard P (1995): Retrospective estimation and correction of physiological fluctuation in functional MRI. Magn Reson Med 34:201–212.

Josephs O, Howseman AM, Friston KJ, Turner R (1997): Physiological noise modelling for multi-slice EPI FMRI using SPM. In: Proceedings of the International Society for Magnetic Resonance in Medicine, Vancouver, B.C., Canada.

Just MA, Cherkassky VL, Keller TA, Minshew NJ (2004): Cortical activation and synchronization during sentence comprehension in high-functioning autism: Evidence of underconnectivity. Brain 127 (Part 8):1811–1821.

Just MA, Cherkassky VL, Keller TA, Kana RK, Minshew NJ (2007): Functional and anatomical cortical underconnectivity in autism: Evidence from an FMRI study of an executive function task and corpus callosum morphometry. Cereb Cortex 17:951–961.

Kastrup A, Li TQ, Takahashi A, Glover GH, Moseley ME (1998): Functional magnetic resonance imaging of regional cerebral blood oxygenation changes during breath holding. Stroke 29:2641–2645.

Kiviniemi V, Kantola JH, Jauhiainen J, Hyvarinen A, and Tervonen O (2003): Independent component analysis of nondeterministic fMRI signal sources. Neuroimage 19 (2 Part 1):253–260.

Kwong KK, Wanke I, Donahue KM, Davis TL, Rosen BR (1995). EPI imaging of global increase of brain MR signal with breathhold preceded by breathing O_2. Magn Reson Med 33:448–452.

Laufs H, Krakow K, Sterzer P, Eger E, Beyerle A, Salek-Haddadi A, Kleinschmidt A (2003): Electroencephalographic signatures of attentional and cognitive default modes in spontaneous brain activity fluctuations at rest. Proc Natl Acad Sci USA 100:11053–11058.

Leopold DA, Murayama Y, Logothetis NK (2003): Very slow activity fluctuations in monkey visual cortex: Implications for functional brain imaging. Cereb Cortex 13:422–433.

Li TQ, Kastrup A, Takahashi AM, Moseley ME (1999): Functional MRI of human brain during breath holding by BOLD and FAIR techniques. Neuroimage 9:243–249.

Lowe MJ, Mock BJ, Sorenson JA (1998): Functional connectivity in single and multislice echoplanar imaging using resting-state fluctuations. Neuroimage 7:119–132.

Lund TE (2001): fcMRI--mapping functional connectivity or correlating cardiac-induced noise? Magn Reson Med 46:628–629.

Lund TE, Madsen KH, Sidaros K, Luo WL, Nichols TE (2006): Non-white noise in fMRI: Does modelling have an impact? Neuroimage 29:54–66.

McKay LC, Evans KC, Frackowiak RS, Corfield DR (2003): Neural correlates of voluntary breathing in humans. J Appl Physiol 95:1170–1178.

McKeown MJ, Sejnowski TJ (1998): Independent component analysis of fMRI data: Examining the assumptions. Hum Brain Mapp 6:368–372.

McKeown MJ, Makeig S, Brown GG, Jung TP, Kindermann SS, Bell AJ, Sejnowski TJ (1998): Analysis of fMRI data by blind separation into independent spatial components. Hum Brain Mapp 6:160–188.

McKeown MJ, Hansen LK, Sejnowsk TJ (2003): Independent component analysis of functional MRI: What is signal and what is noise? Curr Opin Neurobiol 13:620–629.

Minka TP (2000): Automatic choice of dimensionality for PCA. Technical Report 514, MIT Media Lab Vision and Modeling Group.

Muller RA (2007): The study of autism as a distributed disorder. Ment Retard Dev Disabil Res Rev 13:85–95.

Perlbarg V, Bellec P, Anton JL, Pelegrini-Issac M, Doyon J, Benali H (2007): CORSICA: correction of structured noise in fMRI by automatic identification of ICA components. Magn Reson Imaging 25:35–46.

Raichle ME, MacLeod AM, Snyder AZ, Powers WJ, Gusnard DA, Shulman GL (2001): A default mode of brain function. Proc Natl Acad Sci USA 98:676–682.

Rogers BP, Morgan VL, Newton AT, Gore JC (2007): Assessing functional connectivity in the human brain by fMRI. Magn Reson Imaging 25:1347–1357.

Sonuga-Barke EJ, Castellanos FX (2007): Spontaneous attentional fluctuations in impaired states and pathological conditions: A neurobiological hypothesis. Neurosci Biobehav Rev 31:977–986.

Stillman AE, Hu X, Jerosch-Herold M (1995): Functional MRI of brain during breath holding at 4 T. Magn Reson Imaging 13:893–897.

Thomason ME, Burrows BE, Gabrieli JD, Glover GH (2005): Breath holding reveals differences in fMRI BOLD signal in children and adults. Neuroimage 25:824–837.

Van den Aardweg JG, Karemaker JM (2002): Influence of chemoreflexes on respiratory variability in healthy subjects. Am J Respir Crit Care Med 165:1041–1047.

Vincent JL, Patel GH, Fox MD, Snyder AZ, Baker JT, Van Essen DC, Zempel JM, Snyder LH, Corbetta M, Raichle ME (2007): Intrinsic functional architecture in the anaesthetized monkey brain. Nature 447:83–86.

Wise RG, Ide K, Poulin MJ, Tracey I (2004): Resting fluctuations in arterial carbon dioxide induce significant low frequency variations in BOLD signal. Neuroimage 21:1652–1664.